Parallel imaging/manipulation force microscopy

H. Xie,[a] D. S. Haliyo, and S. Régnier
Institut des Systèmes Intelligents et de Robotique, Université Pierre et Marie Curie/CNRS, 4 Place Jussieu, 75005 Paris, France

(Received 30 January 2009; accepted 25 March 2009; published online 14 April 2009)

Conventional atomic force microscope nanomanipulation is inefficient because of the serial imaging/manipulation operation. We present here a parallel imaging/manipulation force microscope (PIMM) to improve manipulation efficiency. The PIMM is equipped with two individually actuated cantilevers with protrudent tips. One cantilever acts as an imaging sensor by scanning nano-objects and tip of the other cantilever that is used as a manipulating tool. Two manipulation schemes were introduced to fulfill parallel imaging/manipulation tasks with normal and high-speed image scan, respectively. Performance of the PIMM was validated by the parallel imaging/manipulation of nanoparticles to form a nanopattern with a commonly used pushing operation. © *2009 American Institute of Physics*. [DOI: 10.1063/1.3119686]

After nanomanipulation achieved with a scanning tunneling microscope in 1990,[1] various nanomanipulation and nanoassembly schemes and systems have been introduced. So far, conventional atomic force microscope (AFM) has been widely applied for the manipulation of nanoparticles (zero-dimensional),[2–6] nanowires (one-dimensional)[7,8] or nanotubes (one- or two-dimensional)[9–11] generally using pushing or pulling operations within a single surface. Unlike nanomanipulation performed in a scanning electron microscope (SEM) and a transmission electron microscope, an inherent limitation of AFM-based nanomanipulation is that the AFM acts as an imaging sensor as well as a manipulation tool, and so cannot provide manipulation with real-time visual feedback, but rather an insufficient serial process of scanning-manipulation scanning.[12] In order to facilitate nanomanipulation, haptic devices and virtual reality interfaces were introduced into AFM-based nanomanipulation systems,[13,14] thereby enabling an operator to directly interact with the real nanoworld. However, the time-consuming scanning-manipulation-scanning operation is still required, making mass production impossible, although virtual reality could provide users with a so-called "visualized" feedback using local scan to update a model-based virtual environment.[14] On the other hand, high-speed AFMs have succeeded in raising the scanning efficiency.[15–18] In this case, the excellent imaging potential of high-speed AFM will be greatly reduced if it is used for nanomanipulation with such a serial scanning-manipulation-scanning process.

The central problem in speeding up AFM-based nanomanipulation is in fact to develop sufficient harmony between image scan and manipulation processes. Like manipulation under optical microscopes or electron microscopes, the classical parallel imaging/manipulation method still offers promise for improving the efficiency of AFM-based nanomanipulation.

Here, we present a parallel imaging/manipulation force microscope (PIMM) to improve the efficiency of AFM-based nanomanipulation. As shown in Fig. 1, the PIMM consists of two sets of similar devices commonly used in a conventional AFM, including two cantilevers with corresponding nanopositioning devices and laser measuring systems. Cantilever I (left), used as an imaging sensor, is fixed on an *X-Y-Z* piezotube (PI P–153.10 H). Hysteresis of the piezotube is well compensated on each axis by the Prandtl–Ishlinskii operator.[19] In order to effectively avoid hysteresis and creep of the piezoactuator, a closed-loop *X-Y-Z* piezoactuated nanostage (MCL Nano–Bio2 M) is used to actuate cantilever II (right), which is mounted on an *X-Y-Z* manual microstage for coarse positioning, and mainly used as a manipulating end effector. In order to achieve this parallel imaging/manipulation task, system control software with two parallel threads was developed to coordinate actions on these two cantilevers.

A key component of the parallel imaging/manipulation force microscope (PIMM), as shown in the left-bottom inset of Fig. 1, is the special cantilever with a protrudent tip that makes interactions between cantilever I and cantilever II feasible. The protrudent tip enables image scan on the tip of cantilever II (tip II) using cantilever I. By this means, the

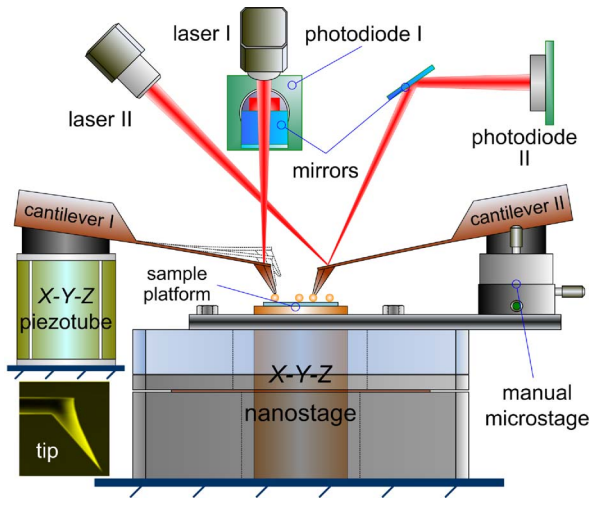

FIG. 1. (Color online) Schematic diagram of the PIMM. The PIMM mainly consists of two individually actuated cantilevers with protrudent tips (left inset). Cantilever I is fixed on the *X-Y-Z* piezotube, which acts as an imaging sensor to provide position information of nano-objects and the tip end of cantilever II. Cantilever II, fixed on the *X-Y-Z* nanostage, is used as a manipulation tool to push and pull nano-objects.

[a]Electronic mail: xie@robot.jussieu.fr.

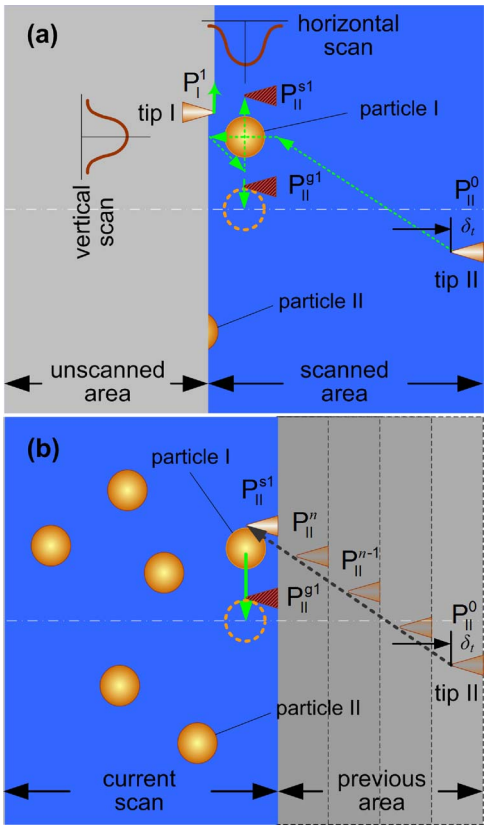

FIG. 2. (Color online) Parallel imaging/manipulation schemes. (a) Parallel imaging/manipulation scheme with normal-speed image scan. In this case, the manipulation is controlled based on the image of the previous scanned area. (b) Parallel imaging/manipulation strategy with high-speed image scan on tip I. By this means, the manipulation is monitored by a high-speed image feedback. The dynamic scan area is shifted by tracking the motion of tip II to keep a fixed scan length δ_t on tip II.

relative positions between nano-objects and tip II end can be obtained from the image scan that is indispensable for AFM-based manipulation. The tilted angle of the cantilever tip is approximately 62°–64° on the side view without a mounting angle. In the PIMM, the cantilevers are mounted with an angle of 8°. An excellent image quality can be achieved even though the scan length on tip II is more than 300 nm, which is sufficient for tip positioning with a dynamic image display updated by real-time scanning data.

Figure 2(a) is a diagram of the parallel image/manipulation with a normal-speed image scan using tip I. First, each axis of the nanostage and the piezotube is initialized in its proper position, which should provide an enough motion range for the nanomanipulation within an image scanning area. The next step is to locate tip II by local scan of tip II using tip I. Once tip II locating is ready, two parallel threads are started to perform a parallel imaging/manipulation task. One is used to control tip I to fulfill a full scan of the pertinent area selected under a optical microscope, resulting in a topographic image containing of nano-objects to be manipulated as well as tip II end (as a simulated image on position P_{II}^{0}). The second thread is assigned to dominate the performance of tip II, which is in idle process until a particle emerges on the dynamic image display. As particle I is entirely scanned while tip I reaches position P_{I}^{1}, the first manipulation is started after the coarse position of particle I is estimated by processing the dynamic image of the scanned area. In order to obtain an accurate position of particle I, tip II locally scans the nanoparticle horizontally and vertically along a line marked on Fig. 2(a) to locate the precise center of the nanoparticle and estimate the contact point between the tip and the nanoparticle. As tip II reaches P_{II}^{s1}, the manipulation is started until tip II reaches P_{II}^{g1} where particle I has been pushed to the target position. After the first manipulation, tip II is set to idle process again until the particle II emerges within the dynamic image.

Figure 2(b) shows another strategy of the parallel imaging/manipulation with a high-speed image scan using tip I. As in the steps discussed above, once system initialization and local scanning on tip II are ready, the parallel image/manipulation task is started. Tip I is used for high-speed image scan of nano-objects and tip II end, producing a high-speed topographic image display which consists of tip II and nano-objects to be manipulated. Tip II started to approach particle I for the first manipulation after the first frame of the dynamic image display. Simultaneously, the scan area is dynamically shifted by tracking the motion of tip II to keep a fixed scan length δ_t on tip II for a purpose of avoiding a block of the image scan due to excessive scan height on tip II. The scan area is moved from P_{II}^{0} to P_{II}^{n} until tip II reaches P_{II}^{s1}, at which point the manipulation is started to laterally push particle I until tip II reaches P_{II}^{g1}. After the first manipulation, tip II is moved on to the next nanoparticle.

Task time t_{task} of the parallel imaging/manipulation operation can be given as

$$t_{\mathrm{task}} = \max(t_s, t_m) + t_s, \tag{1}$$

where t_s is scanning time of one image frame and t_m is total manipulation time estimated from the sum of manipulation time of each single nano-object. For the normal-speed AFM, t_{task} is often equal to $2t_s$ except for a complex manipulation task that cannot be fulfilled within one frame period and so has task time of t_m+t_s. This scheme can save much time, as compared with the serial imaging/manipulation operation that has task time of t_m+2t_s. One disadvantage of this scheme is that environment-based motion planning is unavailable during the manipulation. However, the parallel imaging/manipulation can be perfectly performed by this scheme if a manipulation objective is defined before the operation. In contrast, for the second scheme, the task time with the high-speed AFM is approximately equal to t_m due to very high frame rate of image scan. The manipulation process in this scheme is monitored by the high-speed visual feedback as the manipulation performed in the SEM. The second scheme is undoubtedly more efficient than the former one.

High-speed image scan is not yet available on the current system. However, a parallel image/manipulation task was performed with a normal-speed image scan on the PIMM we developed. Manipulation results are shown in Fig. 3, in which four Ag nanoparticles with a diameter of 74–82 nm, emerged on dynamic image I–IV in sequence, were pushed onto the image midline during the image scan. In the experiment, the frame period was about 10 min. In contrast, the total manipulation time of these four nanoparticles was less than 1 min with a pushing velocity of about 300 nm/s. These results indicate that we can complete a more complex manipulation task during the image scanning thread to greatly increase the efficiency of the AFM-based nanomanipulation and making mass production feasible.

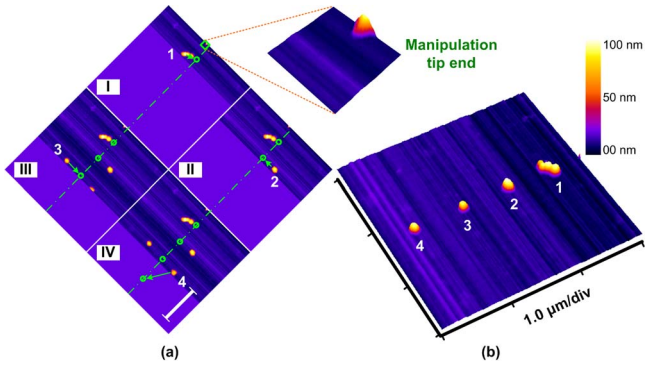

FIG. 3. (Color online) A parallel imaging/manipulation result with a normal-speed image scan using tip I. (a) Emergences of four particles (with a diameter of 74–82 nm) on four different dynamic displays, namely, image I–IV. Once one particle has been fully scanned, a corresponding manipulation task will be started to push it to its destination. (b) A manipulation result. These four nanoparticles were pushed along a line within the frame period of the image scan. The total manipulation time for these four particles was less than 1 min, which is much less than the entire imaging time of 10 min.

In addition, use of the PIMM we developed can be extended to other potential applications. For example, as shown in Fig. 4, a nanotweezer, constructed from the same tips with minor modification to the current system setup, could be used to achieve pick-and-place nanomanipulation. This application will be of considerable interest because of its three-dimensional manipulation capabilities at the nanoscale. It could also be used for real-time force sensing during the manipulation, which will be of significant interest to researchers working in the field of the force spectroscopy, such as nanowire peeling force spectroscopy.[20]

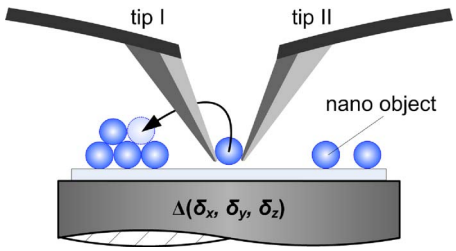

FIG. 4. (Color online) Pick-and-place nanomanipulation using the PIMM we developed with a minor modification to build a nanotip nanotweezer.

In summary, we have developed a PIMM to speed up the AFM based nanomanipulation. We also introduced two manipulation schemes based on normal-speed and high-speed image scan. An experimental result validated the parallel imaging/manipulation scheme with normal-speed image scan. Moreover, for the PIMM, many surprising achievements will be made possible if high-speed image scan is available, and its potential applications are explored in future work.

This work has been supported by the French National Agency of Research through the NANOROL project. The authors would like to thank Professor L. X. Dong from Michigan State University for helpful discussions on AFM-based parallel nanomanipulation.

[1]D. M. Eigler and E. K. Schweizer, Nature (London) **344**, 524 (1990).
[2]T. Junno, S. B. Carlsson, H. Q. Xu, L. Montelius, and L. Samuelson, Appl. Phys. Lett. **72**, 548 (1998).
[3]M. Martin, L. Roschier, P. Hakonen, U. Parts, M. Paalanen, B. Schleicher, and E. I. Kauppinen, Appl. Phys. Lett. **73**, 1505 (1998).
[4]R. Resch, D. Lewis, S. Meltzer, N. Montoya, B. E. Koel, A. Madhukar, A. A. G. Requicha, and P. Will, Ultramicroscopy **82**, 135 (2000).
[5]D. Dietzel, T. Mönninghoff, L. Jansen, H. Fuchs, C. Ritter, U. D. Schwarz, and A. Schirmeisen, J. Appl. Phys. **102**, 084306 (2007).
[6]L. M. Tong, T. Zhu, and Z. F. Liu, Appl. Phys. Lett. **92**, 023109 (2008).
[7]X. D. Li, H. S. Gao, C. J. Murphy, and K. K. Caswell, Nano Lett. **3**, 1495 (2003).
[8]S. Samitsu, T. Shimomura, K. Ito, M. Fujimori, S. Heike, and T. Hashizume, Appl. Phys. Lett. **86**, 233103 (2005).
[9]M. R. Falvo, R. M. Taylor, A. Helser, V. Chi, F. P. Brooks, Jr., S. Washburn, and R. Superne, Nature (London) **397**, 236 (1999).
[10]M. Prior, A. Makarovski, and G. Finkelstein, Appl. Phys. Lett. **91**, 053112 (2007).
[11]P. M. Albrecht and J. W. Lyding, Small **3**, 146 (2007).
[12]L. X. Dong and B. J. Nelson, IEEE Rob. Autom. Mag. **14**, 111 (2007).
[13]S. G. Kim and M. Sitti, IEEE Trans. Autom. Sci. Eng. **3**, 240 (2006).
[14]G. Y. Li, N. Xi, H. P. Chen, C. Pomeroy, and M. Prokos, IEEE Trans. Nanotechnol. **4**, 605 (2005).
[15]G. E. Fantner, P. Hegarty, J. H. Kindt, G. Schitter, G. A. G. Cidade, and P. K. Hansma, Rev. Sci. Instrum. **76**, 026118 (2005).
[16]P. K. Hansma, G. Schitter, G. E. Fantner, and C. Prater, Science **314**, 601 (2006).
[17]Y. Seo, C. S. Choi, S. H. Han, and S.-J. Han, Rev. Sci. Instrum. **79**, 103703 (2008).
[18]J. P. Howard-Knight and J. K. Hobbs, Appl. Phys. Lett. **93**, 104101 (2008).
[19]P. Krejci and K. Kuhnen, IEE Proc.: Control Theory Appl. **148**, 185 (2001).
[20]M. C. Strus, L. Zalamea, A. Raman, R. B. Pipes, C. V. Nguyen, and E. A. Stach, Nano Lett. **8**, 544 (2008).